WATT-CLASS CONTINUOUS WAVE Er^{3+}/Yb^{3+} FIBER AMPLIFIER

by

MAY EBBENI

B.A., Yarmouk University, 2006

A REPORT

submitted in partial fulfillment of the requirements for the degree

MASTER OF SCIENCE

Department of Physics
College of Arts and Sciences

KANSAS STATE UNIVERSITY
Manhattan, Kansas

2012

Approved by:

Major Professor
Brian R. Washburn

Copyright

Abstract

Rare-earth doped optical fibers can be used to make optical amplifiers in the near infrared with large optical gain in an all fiber based system. Indeed, erbium doped fibers made gain possible within the 1532 to 1560 nm band which makes long span fiber optical communication systems a possibility. Erbium doped fibers have also been used to make narrow linewidth or mode-locked lasers. Other rare-earth doped fibers can be used for amplifiers in other near-infrared spectral regions. Recently, fiber amplifier technology has been pushed to produce watt level outputs for high power applications such as laser machining. These high power amplifiers make new experiments in ultrafast fiber optics a possibility.

This report reviews the current literature on Watt-class continuous wave erbium doped amplifiers and discussed our attempt to develop a high power Yb/Er amplifier. After the design of the cladding pump in 1999, the world's first single mode fiber laser with a power greater than 100 Watts of the continuous wave light was introduced. After 2002 there was a huge spike in the output powers (up to 2 kW) of lasers based on rare-earth doped fibers. Our own work involved developing a 10 W amplifier at 1532 nm and 1560 nm. A high power amplifier was made by seeding a dual-clad Yb/Er co-doped fiber pumped at 925 nm using a lower power erbium doped fiber amplifier. We will discuss the design and construction of the amplifier, including the technical difficulties for making such an amplifier.

Table of Contents

List of Figures

Acknowledgements

I would like to express my sincerest gratitude to my supervisor Dr. Brian Washburn, to whom I will always be indebted, for his inestimable help and guidance throughout the MSc course and during the dissertation stage. I would also like to extend my deepest appreciation to Dr. Kristan Corwin for taking interest in this project and guiding me at all the time when I needed.

I am thankful to my committee members Dr. Washburn, Dr. Kristan and Dr. Kumarappan who were willing to accept my defense schedule in spite of their busy schedule.

I would like to thank all the group members, special thanks to Dr. Will Hageman for his great help in this project, Andrew Jones for his help and discussions, Rajesh Kadel, Shun Wu and Chenchen Wang for being great partners in the lab. I would like to thank our previous group member Dr. Jinkang Lim; I used to take a lot of his time when I first joined the group and he was always willing to help out and to explain the things for me. I am thankful to the people working in JRM lab for providing me the good and healthy atmosphere to do research.

At the end I would like to thank my parents for their unconditional support and love. I'm thankful for their prayers, in the day and the middle of the night.

This work was supported by the Air Force Office of Scientific Research (FA9550-08-1-0344).

Dedication

To my parents; Hussien Ebbeni and Sarab Haris.

Chapter 1 - Introduction

There are many advantages to building a laser or an amplifier consisting only of optical fibers and fiber-based optical components. The light will be guided in the fiber so there will be no need for any careful alignments. Fiber-based laser systems or amplifiers designs are robust and compact, therefore they are mobile, stable and at lower coast.

The eye safe spectral region of the mid-infrared (MIR) offers high transmission in the atmosphere which is essential to many applications such as remote sensing and space-based terrestrial imaging and communications. For that, the need for portable and tunable lasers working in the MIR is increasing. A new class of optically pumped gas laser based on population inversion was recently presented [1], where acetylene (C_2H_2) gas is confined to a hollow core photonic crystal fiber. Acetylene gas was chosen because of its availability and having its vibration and rotational energy levels well known and documented. The laser produced light near 3 μm when pumped around 1.5 μm [1]. This new class MIR gas laser gives the potential of having robust, efficient and compact step-tunable eye-safe radiation which is needed for a number of applications.

The P13 absorption line of acetylene corresponds to 1532 nm [2]. In order to get this gas laser to operate, we need a high power pump light. Our goal and interest in this project is to amplify a laser signal at around 1535 nm to high powers (up to 10 Watts) in order to be used as a pump for the afore mentioned acetylene gas laser.

Rare earth metal doped fiber lasers and amplifiers are of a great interest for their wide applications in telecommunications (like networks, free space opto-communications [3] and as amplifiers for cable TV [4]), in the medical field and in industry (watts of amplified light for machining). These lasers or amplifier systems are known to have excellent beam quality, efficient heat dissipation and high efficiency as well as being compact and robust. All these qualities make them an alternative to solid state high power lasers.

Erbium doped fibers (EDF's) are known for the wide range of wavelengths at which they absorb and also emit light. Erbium doped fibers are also known for their good transmission at 1550 nm which corresponds to a low-loss transmission window of optical fiber communications [23]. These qualities and more make EDF's of more interest.

First we will discuss basic laser theory, and then introduce erbium doped fibers as well as erbium/ytterbium co-doped fibers in the next chapter including the properties of their emission and absorption spectrums. In chapter 3 a literature reviews followed. Chapter 4 will be about the experiment and the high power amplifier setup followed by the conclusion in Chapter 5.

Chapter 2 - Background

The principle of amplifying the intensity of a laser beam is very similar to the lasers principle itself. Light is amplified through stimulated emission of radiation. Therefore, we would still need a gain medium and build up a population inversion through pumping it with a suitable wavelength of light. See Fig. 2.1.

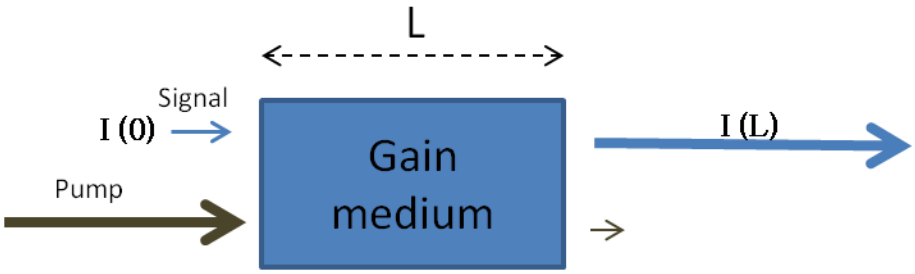

Figure 2.1: Laser light (the Signal) being amplified by the propagation of the pump light through the gain medium for a distance L.

In this chapter, the complex susceptibility is derived through the classical spring model. The importance of the complex susceptibility is later shown within the derivation of the gain which is the key behind amplification of laser light.

The high power amplifier we were trying to build consists of two parts, a pre-amplifier using an erbium doped fiber and a power amplifier where an erbium-ytterbium co-doped fiber was used. At the end of this chapter both of these fibers are also discussed.

2.1 **Complex susceptibility [7]**

In the classical model, the dielectric mediums are the collection of the identical and fix electron oscillators, in which the Coulomb force of attraction is modeled as the spring between the electronic cloud and the nuclei. Figure 2.2 shows a single oscillator located at a certain position z in the material and oriented along the *x-axis*. A uniform plane wave, assumed to be linearly polarized along x - axis, propagates in the material in the z direction.

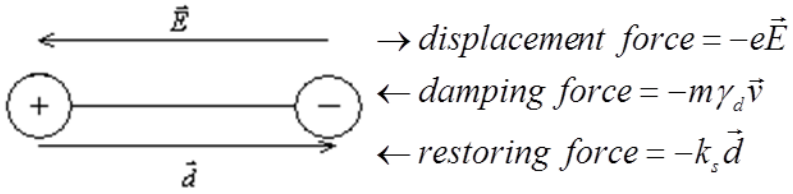

Figure 2.2: A dipole moment of a single oscillator model where the Coulomb force acting upon the positive and the negative charges is being modeled by a spring having a spring constant k_s. The applied electric field displaces the electron through distance d.

The electric field in the wave displaces the electron of the oscillator in the x-direction through a distance represented by the vector $\vec{d}$; a dipole moment $\vec{p}$ is thus established

$$\vec{p}(z,t) = -e\,\vec{d}(z,t) \tag{2.1.1}$$

And the applied force is given by (where e is a positive number):

$$\vec{F}_a(z,t) = -e\,\vec{E}(z,t) \tag{2.1.2}$$

We need to remember that this electric field $\vec{E}(z,t)$ is the vector sum of the applied electric field at each point in space and time and the radiated field from all the other oscillators. The relative phase differences between oscillators can be accurately determined by the spatial and temporal behavior of $\vec{E}(z,t)$.

In a linear medium, the restoring force on the electron $\vec{F}_r$ is produced by a "spring" having a spring constant k_s. According to Hook's Law:

$$\vec{F}_r(z,t) = -k_s\vec{d}(z,t) \tag{2.1.3}$$

The negative sign shows that the restoring force is in the opposite directions to that of the displacement of the electron from the mean position which is the nucleus in this case. If the field is turned off the electron is released and will oscillate (as shown in the figure 2.3) about the nucleus at the resonant frequency, given by the following expression, where m_e is the mass of the electron:

$$\vec{F}_r = m_e \vec{a}$$
$$\Rightarrow k_s d(z,t) = m_e \omega_0{}^2 d(z,t) \tag{2.1.4}$$
$$\Rightarrow \omega_0 = \sqrt{\frac{k_s}{m_e}}$$

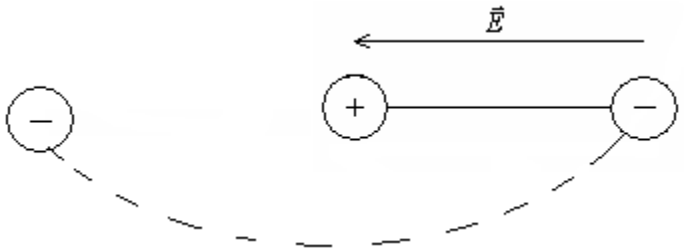

Figure 2.3: Oscillation of the electron about the nucleus

The electron experience damping from the neighboring oscillators, this damping can be modeled by a velocity dependent damping force given by

$$\vec{F}_d(z,t) = -m\gamma_d \vec{v}(z,t) \tag{2.1.5}$$

where $\vec{v}(z,t)$ is the velocity of the electron. Note that from now onward we are going to drop the subscript (e) from the mass (m) since the electrons are the oscillating objects.

By applying Newton's second law of motion and writing down the vector sum of all the forces (damping, applied and restoring) equal to the product of the mass of the electron and its acceleration,

$$m\vec{a} = \vec{F}_a + \vec{F}_r + \vec{F}_d$$
$$\Rightarrow m\frac{\partial^2 \vec{d}_c}{\partial t^2} + m\gamma_d \frac{\partial \vec{d}_c}{\partial t} + k_s \vec{d}_c = -e\vec{E}_c \tag{2.1.6}$$

Where $\vec{E}_c$ is the complex form of the electric field at point (z,t), which includes applied and radiated field as discussed already. Its general form is given as:

$$\vec{E}_c = \vec{E}_0 e^{-ikz} e^{i\omega t} \tag{2.1.7}$$

While the system is being excited by the complex electric field $\vec{E}_c$, one can anticipate a displacement wave $\vec{d}_c$ of the form

$$\vec{d}_c = \vec{d}_0 e^{-ikz} e^{i\omega t}$$
$$\vec{d}_c = \vec{d}_s e^{i\omega t} \tag{2.1.8}$$

Where

$$\vec{d}_s = \vec{d}_0 e^{-ikz} \tag{2.1.9}$$

Putting equations (2.1.7) and (2.1.8) in equation (2.1.6) one can get:

$$m(i\omega)(i\omega)\left(\vec{d}_0 e^{-ikz} e^{i\omega t}\right) + m\gamma_d (i\omega)\left(\vec{d}_0 e^{-ikz} e^{i\omega t}\right) + k_s\left(\vec{d}_0 e^{-ikz} e^{i\omega t}\right) = -e\vec{E}_0 e^{-ikz} e^{i\omega t} \tag{2.1.10}$$

Dividing by $me^{i\omega t}$, and putting $\vec{d}_s = \vec{d}_0 e^{-ikz}$, $\vec{E}_s = \vec{E}_0 e^{-ikz}$ and $\omega_0{}^2 = \frac{k_s}{m}$ the simplified version of this equation is

$$\vec{d}_s\left[-\omega^2 + i\omega\gamma_d + \omega_0{}^2\right] = -\frac{e}{m}\vec{E}_s \tag{2.1.11}$$

Making $\vec{d}_s$ as subject, the resulting equation takes the form,

$$\vec{d}_s = \frac{-\left(e/m\right)}{\left(\left(\omega_0{}^2 - \omega^2\right)^2 + \omega^2\gamma_d{}^2\right)}\vec{E}_s \tag{2.1.12}$$

The dipole associated with the displacement $\vec{d}_s$ is

$$\vec{p}_s = -e\,\vec{d}_s \tag{2.1.13}$$

Assuming that all the dipoles are identical in the medium, and that we have *N* number of dipoles, the polarization vector of the medium can be written as:

$$\vec{P}_s = N\,\vec{p}_s = -e\,N\,\vec{d}_s \tag{2.1.14}$$

$$\Rightarrow \vec{P}_s = \frac{N\left(e^2/m\right)}{\left(\left(\omega_0{}^2 - \omega^2\right)^2 + \omega^2\gamma_d{}^2\right)}\vec{E}_s \tag{2.1.15}$$

But we know that $\vec{P} = \chi\varepsilon_0\vec{E}$, and by comparing this to (2.1.15) we find that the susceptibility of the medium is given by:

$$\chi_{res} = \frac{Ne^2}{\varepsilon_0 m\left(\left(\omega_0{}^2 - \omega^2\right)^2 + \omega^2 \gamma_d{}^2\right)} \tag{2.1.16}$$

Which is a complex number having a real and an imaginary part which are χ'_{res} and χ''_{res} respectively. Thus χ_{res} can be written as

$$\chi_{res} = \chi'_{res} - i\chi''_{res} \tag{2.1.17}$$

Where

$$\begin{aligned} \chi'_{res} &= \frac{Ne^2\left(\omega_0{}^2 - \omega^2\right)}{\varepsilon_0 m\left(\left(\omega_0{}^2 - \omega^2\right)^2 + \omega^2 \gamma_d{}^2\right)} \\ \chi''_{res} &= \frac{Ne^2\left(\omega\gamma_d\right)}{\varepsilon_0 m\left(\left(\omega_0{}^2 - \omega^2\right)^2 + \omega^2 \gamma_d{}^2\right)} \end{aligned} \tag{3.2.18}$$

Figure 2.4 shows the plot of the real and the imaginary parts of complex susceptibility. The important points to note in this plot are the symmetric behavior of the χ''_{res} about $\omega = \omega_0$ whose full width half-maximum amplitude is γ_d. Near the resonant frequency where χ''_{res} has a maximum, the wave attenuation (absorption) is at its peak.

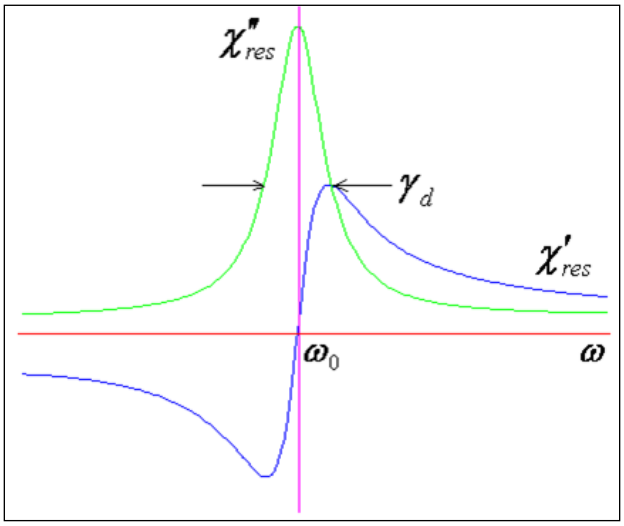

Figure 2.4: Plot of the real and imaginary parts of the resonant susceptibility χ_{res}. The FWHM of the imaginary part χ''_{res} is equal to the damping co-efficient γ_d.

2.2 **Intensity Gain [21]**

In this section, we are going to derive the equation of an electric field propagating in a linear dielectric medium with dielectric constant ε, and a complex susceptibility $\tilde{\chi}_{at}$ which is due to the transitions in the laser atoms in the medium. We are assuming that these atomic transitions are electric-dipole transitions forming an electric polarization $\vec{P}_{\text{at}}$ in the medium.

We know that:

$$\begin{aligned} \vec{B} &= \mu \vec{H} \\ \vec{J} &= \sigma \vec{E} \\ \vec{D} &= \varepsilon \vec{E} + \vec{P}_{\text{at}} = \varepsilon \left[1 + \tilde{\chi}_{at}\right] \vec{E} \end{aligned} \tag{2.2.1}$$

As we know from Maxwell's equations: $\nabla \times \vec{E} = -i\omega \vec{B}$, by taking the curl of this equation we get:

$$\vec{\nabla} \times \left(\vec{\nabla} \times \vec{E}\right) = \vec{\nabla}\left(\vec{\nabla} \cdot \vec{E}\right) - \vec{\nabla}^2 \vec{E} \tag{2.2.2}$$

Assuming that the property of the medium is spatially uniform which means that $\vec{\nabla} \cdot \vec{E} = 0$. And using equation (2.2.1) and the modified Ampere's law: $\vec{\nabla} \times \vec{H} = \vec{J} + i\omega \vec{D}$ we'll get:

$$\vec{\nabla}^2 \vec{E} = i\omega\mu\left(\vec{\nabla} \times \vec{H}\right) = i\omega\mu\left[\sigma + i\omega\varepsilon\left(1 + \tilde{\chi}_{at}\right)\right]\vec{E} = \omega^2 \varepsilon\mu\left[1 + \tilde{\chi}_{at} - i\frac{\sigma}{\omega\varepsilon}\right]\vec{E}$$

$$\left[\vec{\nabla}^2 + \omega^2 \varepsilon\mu\left(1 + \tilde{\chi}_{at} - i\frac{\sigma}{\omega\varepsilon}\right)\right]\tilde{E}(x, y, z) = 0 \tag{2.2.3}$$

Now take a plane wave propagating in the z-direction where $\frac{\partial \tilde{E}}{\partial x} = \frac{\partial \tilde{E}}{\partial y} = 0$, or for a laser beam were $\left|\frac{\partial^2 \tilde{E}}{\partial x^2}\right|$, $\left|\frac{\partial^2 \tilde{E}}{\partial y^2}\right| << \frac{\partial^2 \tilde{E}}{\partial z^2}$, equation (2.2.3) becomes:

$$\left[\frac{d^2}{dz^2} + \omega^2 \varepsilon\mu\left(1 + \tilde{\chi}_{at} - i\frac{\sigma}{\omega\varepsilon}\right)\right]\tilde{E}(z) = 0 \tag{2.2.4}$$

Let

$$\Gamma^2 = -\omega^2 \varepsilon\mu\left(1 + \tilde{\chi}_{at} - i\frac{\sigma}{\omega\varepsilon}\right)$$

$$= -\beta^2\left(1 + \tilde{\chi}_{at} - i\frac{\sigma}{\omega\varepsilon}\right), \quad \text{where} \quad \beta = \omega\sqrt{\varepsilon\,\mu} = \frac{\omega\, n}{c}$$

$$\Rightarrow \Gamma = i\beta\sqrt{\left(1+\tilde{\chi}_{at}-i\frac{\sigma}{\omega\varepsilon}\right)},$$

Since $\tilde{\chi}_{at}$ *and* $\frac{\sigma}{\omega\varepsilon} << 1$ then we can expand the square root:

$$\Gamma = i\beta\left(1+\frac{\tilde{\chi}_{at}}{2}-i\frac{\sigma}{2\omega\varepsilon}\right) = i\beta + i\frac{(\chi' + i\chi'')\beta}{2} + \frac{\beta\sigma}{2\omega\varepsilon}$$

$$\Gamma(\omega) = i\beta + \Delta\beta_m(\omega) - \alpha_m(\omega) + \alpha_0$$

Where:

$$\beta = \omega\sqrt{\varepsilon\mu} = \frac{\omega n}{c}$$

$$\Delta\beta_m(\omega) = \frac{\beta\,\chi'(\omega)}{2}$$

$$\alpha_m(\omega) = \frac{\beta\,\chi''(\omega)}{2}$$

$$\alpha_0 = \frac{\sigma n}{2\varepsilon c}$$

So now we can write the real part of the electric field as a solution of the differential equation

$$\varepsilon(z,t) = \mathrm{Re}\left[\tilde{E}_0\right]\exp\{i\omega t - i(\beta + \Delta\beta_m(\omega))z + (\alpha_m(\omega) - \alpha_0)z\} \tag{2.2.4}$$

But since:

$$\begin{aligned} I(z) &= |\varepsilon(z,t)|^2 \\ \Rightarrow I(z) &= \left(\mathrm{Re}\left[\tilde{E}_0\right]\right)^2 \exp\{2[\alpha_m(\omega) - \alpha_0]z\} \end{aligned} \tag{2.2.5}$$

The intensity gain $G(\omega)$ is defined as the ratio of the output intensity to the input intensity as the following:

$$\boxed{G(\omega) = \frac{I(L)}{I(0)} = \exp\{2[\alpha_m(\omega) - \alpha_0]L\}} \tag{2.2.6}$$

Note that $\alpha_m(\omega)$ is assumed to be greater than α_0 to call this ratio between the output and input intensities as "Gain", otherwise; it would become a "Loss"

2.3 **Saturated Gain [8]**

When a signal wave is propagating along the medium then the amplified light is proportional to the total inversion (ΔN)[1] of the laser atoms. This amplified light grows bigger exponentially with respect to the distance travelled in the medium. However; and since we are dealing with a confined system, then ΔN would reach saturation causing a saturation in the Intensity of the light. This intensity is called I_{sat}.

In order to extract the energy efficiently form the amplifier, the input signal should be intense enough to achieve the desired population inversion when propagating through the gain medium.

If we look back at equation (2.2.5), assuming that α_0 is very small then we can write:

$$\frac{1}{I(z)} \times \frac{dI(z)}{dz} = 2\alpha_m(I) = \frac{2\alpha_{mo}}{1+(I(z)/I_{sat})}$$

Where α_{mo} is the unsaturated gain coefficient.

Rearrange: $$\int_{I_{in}}^{I_{out}} \left[\frac{1}{I} + \frac{1}{I_{sat}}\right] dI = 2\alpha_{mo} \int_{z=0}^{z=L} dz$$

$$\ln\left(\frac{I_{out}}{I_{in}}\right) + \frac{I_{out} - I_{in}}{I_{sat}} = 2\alpha_{mo}L = \ln G_o$$

Where G_o is the small signal gain [$G_o = \exp(2\alpha_{mo}L)$]

By rearranging again: $G \equiv \frac{I_{out}}{I_{in}} = G_o \times \exp\left[-\frac{I_{out} - I_{in}}{I_{sat}}\right]$, and $G_{dB} = 10 \times \log\left[\frac{I_{out}}{I_{in}}\right]$

To explain why the absorption and emission spectra of particularly erbium ions doped in silica fiber will not match we have to consider the following figure. Figure 2.5 shows the transition between two bands whose populations are given by the Boltzmann factor for state within the band. In figure (a) we have erbium ions in thermal equilibrium and in figure (b) pump is used.

---

[1] $\Delta N = (g_2/g_1)N_1 - N_2$ replaces N in equation (2.1.16) where the condition for a population inversion is $(N_2/g_2) > (N_1/g_1)$. N_1 and N_2 are the total populations in energy levels E_1 and E_2 with corresponding degeneracy's g_1 and g_2. The lasing wavelength correspond to the energy difference $E_2 - E_1$

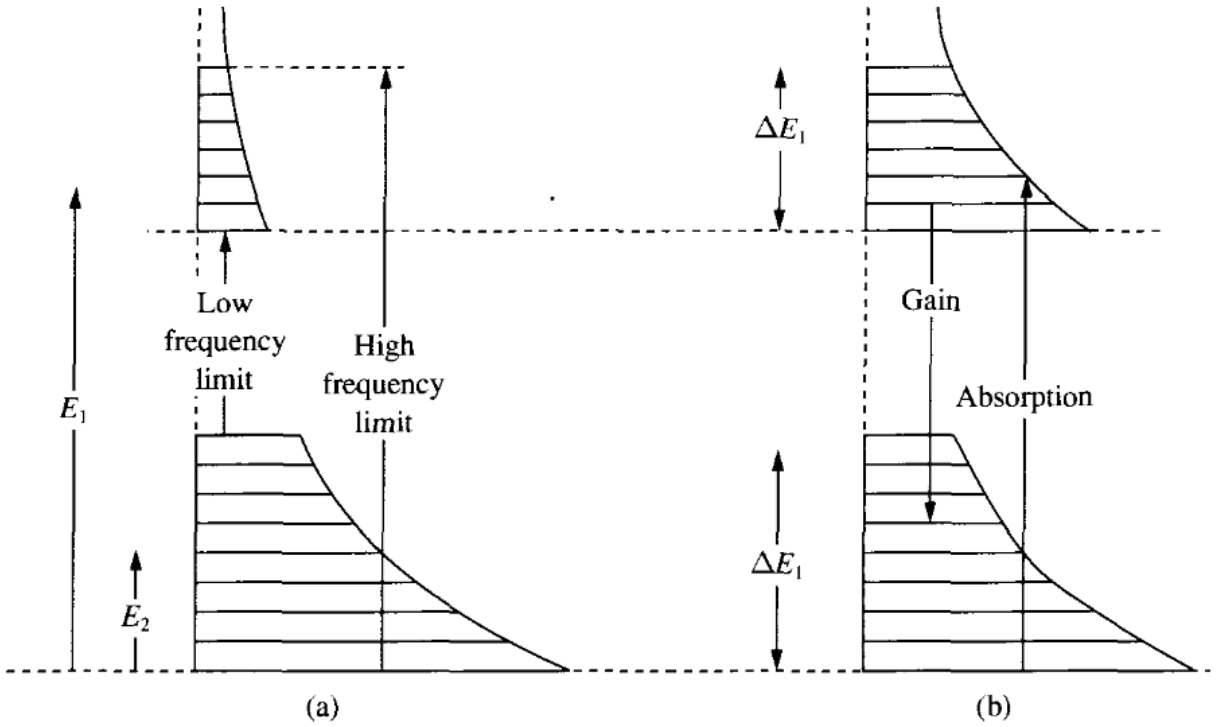

Figure 2.5: Boltzmann distribution for Erbium ions doped in silica fiber in (a) thermal equilibrium. (b) during population inversion. Reproduced from Ref. [5].

Here we can see that in figure 2.5 (a) the upper state manifold is almost empty while the lower state is more populated having a Boltzmann distribution. Hence the absorption coefficient which depends upon frequency will give the information about the relative population of the lower state manifold. It is clear from the figure that the population in the highest state of the lower manifold is less by $exp[-\Delta E_1 / kT]$ as compare to the bottom of the same manifold. This results in small absorption at low frequency.

Considering figure 2.5 (b) where pump is used and population inversion is achieved. Hence there will be non-zero (Boltzmann) distribution of electrons in the upper manifold. This increases the possibility of absorption on the high frequency (short wavelengths). Considering the limitation of the selection rules there can be considerable fluorescence (gain) at the low frequency (long wavelength). Because of this the absorption at the higher frequencies (short wave lengths) is quite considerable. One can see from this explanation why is it harder to get

more gain at the shorter wavelengths while it's relatively easier to get it at the longer wavelengths.

2.4 **Erbium and Ytterbium doped fibers**

The first rare earth metal was discovered more than 200 years ago, but it was only recently that these metals have been used in the industry. That was after the development of some techniques for separating these elements efficiently between the 1950's and 1960's.

When doping an ion in a material (in this case fused-silica) then this dopant would feel the electric field of the surrounding host material, causing the energy levels of this dopant to split due to the Stark effect. As a result of that, the energy levels get broadened. That is very useful since it gives us a more wide range of wavelengths to pump at and also to "lase" upon. Erbium, Ytterbium and Thulium are very common rare-earth metals that had been doped in fused-silica fibers and used for many different applications.

Another advantage of these rare-earth metals is the ability to tune the emission spectrum by different dopants in different hosts. Table 2.1 shows the different wavelengths range for different rare-earth metal ions doped in different hosts.

Rare earth ion	Host glasses	Emission wavelengths
Neodymium (Nd^{+3})	Silicate and phosphate glasses	1.03 – 1.1 μm
Ytterbium (Yb^{+3})	Silicate glass	1.0 – 1.1 μm
Erbium (Er^{+3})	Silicate, phosphate, fluoride glasses	1.5 – 1.6 μm , 2.7 μm
Thulium (Tm^{+3})	Silicate, phosphate, fluoride glasses	1.7 – 2.1 μm, 1.45 – 1.53 μm
Holmium (Ho^{+3})	Silicate, fluorozirconate glasses	2.1 μm, 2.9 μm

Table 2.1: Emission wavelengths of different rare-earth metals ions, doped in different fibers.

The kind of gain mediums we were using for this amplifier are fused-silica fibers doped with Er^{3+} ions in one part and co-doped with Er^{3+} and Yb^{3+} in the second. Next is a description of both:

- Er^{3+} ion doped fiber:

It was discovered that the Erbium ion, once doped in silica fused fiber, has a high gain around 1550 nm which is of an interest since it's in the eye-safe region. See Fig. 2.6. Since then, erbium doped fiber lasers and amplifiers have attracted attention for applications in areas such as range finding, free space and satellite telecommunications. It was also found that the erbium doped fibers have a low attenuation around 1550 nm making it very suitable as a fiber amplifier in the C band of the telecommunication systems.

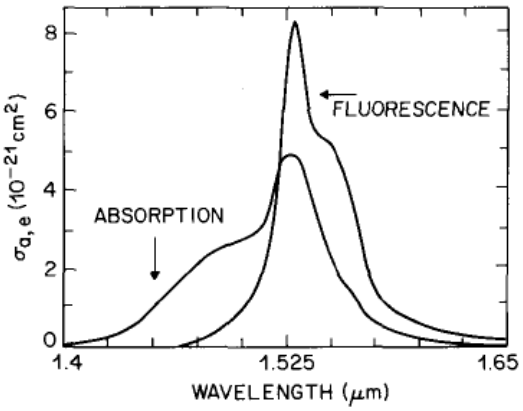

Figure 2.6: Florescence and absorption cross section for Er^{3+} ion around 1525 nm. Reproduced from Ref. [22].

Looking at the figure 2.7 in the next page, we can see the energy levels of the Er^{3+} ions. Due to the Stark effect caused by the silica molecules around the Er^{+3} ions, the energy levels of the ion splits and the degeneracy is then lifted. Pump light at 980 nm or 1480 nm are typically used to pump the Erbium doped fibers.

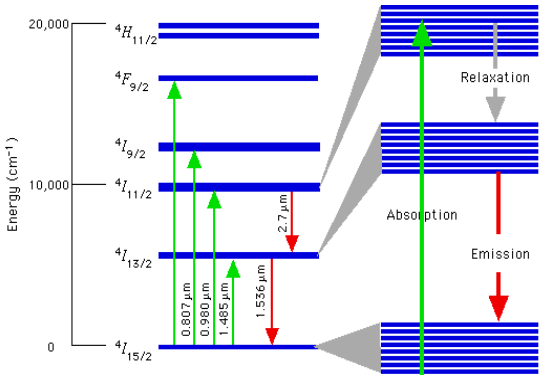

Figure 2.7: Energy levels of Er^{+3} ions. Reproduced from Ref. [6].

Er^{+3} ions are considered as a three level system. Let's take the 980 nm pump light case where the transition ${}^4I_{15/2} \rightarrow {}^4I_{11/2}$ occurs, followed by a quick transfer to the state ${}^4I_{31/2}$ and finally radioactively decays back to ${}^4I_{15/2}$ state. With a relatively extremely long life time of 14ms, this system fulfils the requirements for the production of the desired population inversion.

On the other hand, there are few issues that limit the usage of erbium doped fibers for high power amplifications. Erbium ions tend to clump together in pairs during the diffusion process of the fiber. In result, the erbium ions exchange energy without generating light, thereby limiting the maximum amount of amplification from the fiber.

The surface damage threshold of pure silica is of the order of few GW/cm^2 and even reduced to at least 500 MW/cm^2 for doped silica hosts [9]. The core size of a typical fiber is in the magnitude of few µm. these two facts combined put another limitation for the power produced from fiber based lasers or amplifiers due to the high intensity of the light in the microstructure waveguides.

- <u>Er^{3+}/Yb^{3+} co-doped fiber:</u>

It is hard to achieve efficient pump absorption on the ${}^4I_{15/2} \rightarrow {}^4I_{11/2}$ transition of the Er^{+3} ions due to the relatively small absorption cross sections, add to that the limitations on the doping concentration in order to avoid excessive clumping between the erbium ions. Co-doping with ytterbium ions is a common method to solve this issue.

It was found that co-doping fused-silica fibers with ytterbium and erbium is very useful as it lead to the increase of the pump absorption of the fiber, therefore; the systems efficiency

was increased [20]. Looking at figure 2.8 one can see that the energy between the states $^2F_{5/2}$ and $^2F_{7/2}$ in the Yb^{3+} ion is very close to the energy between the states $^4I_{11/2}$ and $^4I_{15/2}$ in the Er^{3+} ion, and that enables the ytterbium ions to contribute in the building up of the population inversion in the erbium ions between $^4I_{13/2}$ state and $^4I_{15/2}$ state, hence increasing the pump efficiency. The ytterbium ions can efficiently absorb pump light (980 nm for example), and transfer the energy to erbium ions in the ground state bringing them to $^4I_{11/2}$ state. From here the electrons are quickly transferred to the $^4I_{13/2}$ upper laser level state so the energy transfer back to the ytterbium ions is suppressed. See figure 2.8.

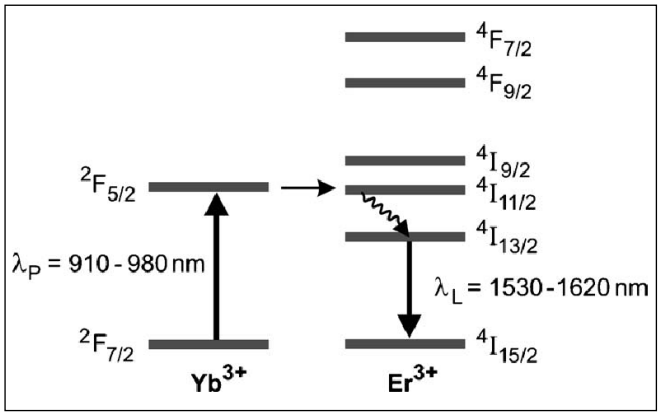

Figure 2.8: Energy diagram of Yb^{3+} and Er^{3+} co-doped in silica. Reproduced from Ref. [20].

If one would try to optimize the EDF's in order to get the maximum amplification efficiency, then the best design leads to the increase in the non-linear effects. The solution of these unwanted non-linearity while keeping the maximum efficiency was found as co-doping the EDF with Yb^{3+} [10] yet another reason to co-dope EDF's with ytterbium.

A down side of this co-doped fiber is the saturation behavior which is related to a bottleneck effect due to the finite Yb to Er transfer rate which causes the reduction in the efficiency at high powers, this arises especially where the pump wavelength near 980 nm is chosen taking advantage of the large Yb^{+3} absorption cross section and maximize the pump rate. However, when the absorption rate of the pump light by the Yb^{+3} ions is higher than the transfer

rate of energy to the Er^{+3} ions, bottle necking effects occurs. Performance can be improved by using new fibers with an increased rare-earth concentration which show negligible signs of erbium clumping.

Chapter 3 - Literature review

As discussed earlier, our goal was to build a high power amplifier up to 10 W at 1532 nm using an erbium/ytterbium co-doped fiber to pump a gas filled hollow core photonic crystal fiber laser in the MIR region. Our interest in the 1532 nm wavelength is due to the P13 strong absorption line of acetylene gas (C_2H_2) which is used in this hollow core gas filled fiber laser.

A study of literature was done mainly focused on high power amplifiers (in order of watts) at wavelengths around 1530 nm to 1540 nm, since these are the pump wavelengths for the molecular gas laser, based on erbium/ytterbium co-doped fibers. Both continuous wave and pulsed amplifiers are illustrated in this chapter. However, very little literature was found about Er/Yb doped fiber amplifiers operating on the wavelength of our interest, in part, since it is difficult to get high gain out of an Er/Yb fiber at this wavelength region..

After the invention of erbium doped fiber amplifiers (EDFA's) by D. N. Payne and coworkers in 1987, long haul optical communication became inexpensive and more reliable. Since then optical fiber became a must for these telecommunication systems. However, in the cases where high powers are needed, an EDFA doesn't work very well when the density of the power increases to the point where it damages to the fiber.

To achieve higher powers, the pump absorption efficiency needed to be increased, co-doping the fused-silica fibers with both erbium and ytterbium found to have achieved this goal. erbium/ytterbium co-doped fibers (EYDF's) with cladding-pumped designs are known to be a suitable choice in the literature for high power fiber amplifiers and lasers operating at wavelengths around the 1550 nm [12].

When building a high power amplifier there are few things to be taken under consideration. First of all is the pump energy. The output of the pump lasers should be higher in power than the output expected from the amplifier. The development of high power semiconductor laser diodes was going on in the recent years and still, and now they are available at different levels of power and as high as hundreds of kilowatts with combined laser diode arrays. The second issue is the fact that high optical powers can damage the fibers. If the optical power inside a fused-silica based fiber exceeds the damage threshold of silica (~5 W/μm^2) then the fiber might be destroyed. Thermal effects can have a significant impact on the system as well

when reaching a high power in the amplifier. Luckily, the geometry of the fibers increases the surface-to-volume ratio making it easier to dissipate the heat along the fiber.

Figure 3.1 shows the absorption and emission spectrum of an erbium/ytterbium co-doped fiber (EYDF). We can see that the EYDF can be pumped around 1540 nm and at the wavelengths between 900 nm and 1000 nm with a very strong absorption at 975 nm. On the other hand, this fiber is suitable to amplify light between 1530 nm to 1560 nm. Notice that the threshold pumps power would be relatively higher in case of pumping in the 1540 nm region due to the high re-absorption at the same pump wavelength. This wide absorption spectrum of Yb^{+3} makes it easy to configure the pump sources. In silica host, the pump wavelength can extend from 800 nm to 1060 nm.

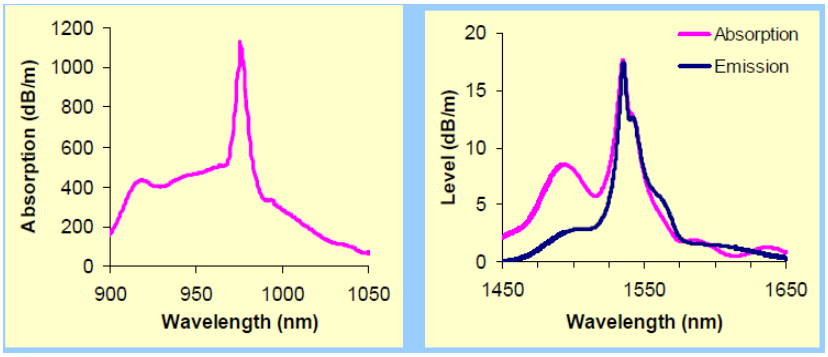

Figure 3.1: Emission and absorption (in pump and signal bands) spectrum for an Er^{+3}/Yb^{+3} co-doped fiber (DF1500Y). Reproduced from Ref. [13].

Yb^{+3} doped fibers have a relatively narrow absorption line at 975 nm and broad emission bandwidths that do not change significantly from one host to another. The ions have relatively long meta-stable lifetime, and yield relatively high quantum efficiency for fiber lasers or amplifiers.

3.1 CW Er/Yb co-doped fiber amplifiers

A demonstration of a high power EYDFA with flattened gain within 0.2 dB over 14 nm was published in 1996. Figure 3.2 below shows the structure of this two-stage amplifier.

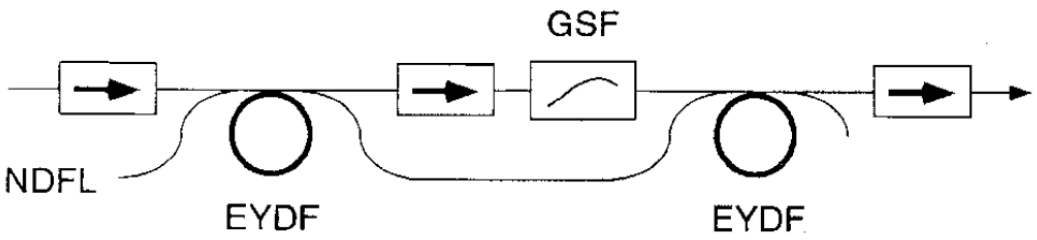

Figure 3.2: two-stage amplifier. EYDF: Erbium-ytterbium doped fiber, NDFL: Neodymium doped fiber laser as a pump source at 1060nm, GSF: gain shaping filter. Reproduced from Ref. [14].

The length of the EYDF in the first stage was 2.5 m, this length was chosen to minimize the noise figure of the total EYDFA. The measured output power was 13 dBm after the first stage with a 0 dBm input signal. For the second stage, the proper choice of the EYDF length and the filter spectrum design are very much related. A flattened gain of 20 dB between 1545 nm and 1560 nm was obtained with a 9.4 m long EYDF at the second stage pumped with 1 W pump power at 1060 nm. This was achieved for different signal powers ranging from -11 dBm to 1 dBm by simply adjusting the pump power. The maximum output power was 24.6 dBm (~290 mW) at 1548 nm [14].

Another set up of a high power amplifier using a dual-clad EYDF was published in 1999. This time the amplifier was pumped using a V groove, side pumping technique which allows efficient pumping of the dual-clad EYDF and a more compact size of the system [15].

The side pumping technique consists of a 90° V groove fabricated on the inner cladding of the dual-clad fiber after being stripped from the polymer coating (a small section was stripped). The pump light is focused on one side of the facet of the V groove using a micro lens. This V groove was located close to one end of the fiber. The fiber was mounted to an AR coated glass substrate where a low refractive index material was used. The incident pump light undergoes total internal reflection at the glass-air interface of the V groove facet to be then guided through the fiber. See figure 3.3. The total diode to fiber coupling efficiency was 84% at the higher pump powers.

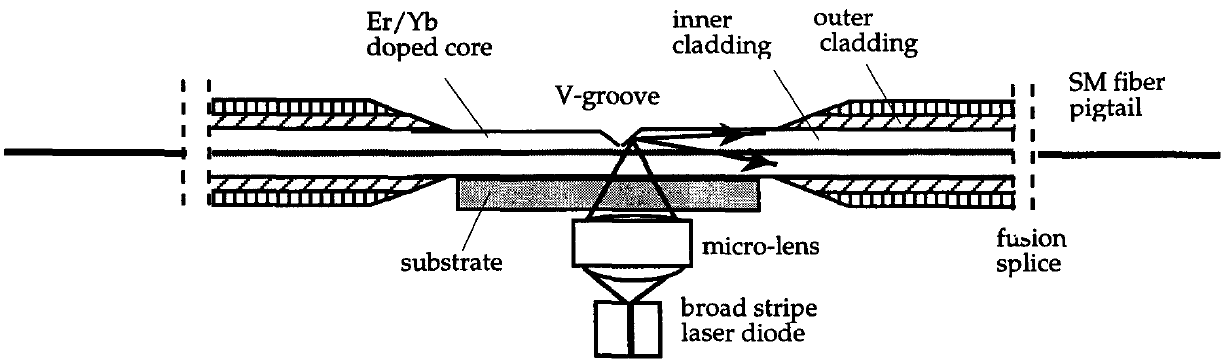

Figure 3.3: Side pumping of the Er/Yb co-doped dual-clad fiber using a V groove. Reproduced from Ref. [15].

Seeded with 8 mW at 1543 nm, the output of the EYDFA had a maximum power of 1.5 W and 1.1 W for the backward and forward pumping respectively. The slope efficiency measured with respect to the absorbed pump power was 48%. The electrical-to-optical conversion efficiency was 15% at highest powers. An output power of 30 dBm (≡ 1 Watt) was found in the case of backward pumping for the wavelengths between 1530 nm and 1560 nm. the pump current was at 5 A and the input power was 9 dBm [15].

Figure 3.4 shows yet another setup of a pre-amplifier followed by a power amplifier. The output of this set up went up to more than 3 W.

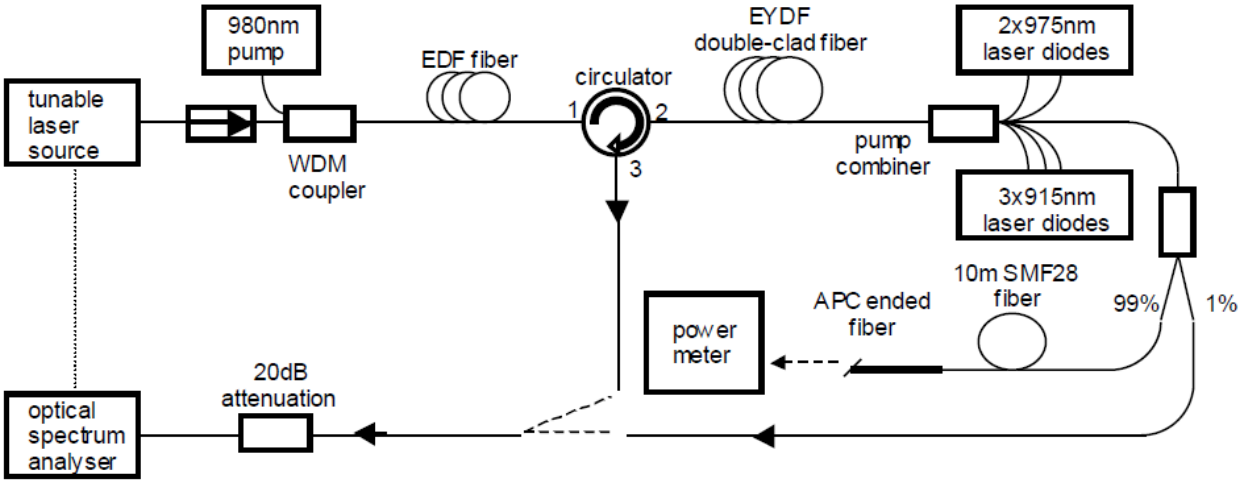

Figure 3.4: Experimental setup of a erbium doped fiber amplifier followed by a power erbium-ytterbium co-doped fiber amplifier. Reproduced from Ref. [16].

The pre-amplifier is an EDFA using a highly erbium doped single mode fiber, with a length of 1.8 m. it was forward pumped with 200 mW pump power at 980 nm. Between the pre-amplifier and the following power amplifier an optical circulator was added. It is to ensure an optical isolation and to allow monitoring the ASE and back scattered C-band signals as well using an optical spectrum analyzer. The power amplifier consists of a dual-clad EYDF with a backward pump scheme through six low loss multi mode fiber input ports used for pumping and another single mode fiber for seeding purposes. Two laser diodes at 975 nm and three more operating at 915 nm were used to pump the EYDF amplifier.

The pre-amplifier provided a flat gain and output power of at least 45 mW between 1540 nm to 1570 nm with a maximum of almost 54 mW at 1560 nm. The overall design provided flat gain with output power higher than 33 dBm in a wide band of 1545 nm to 1570 nm with a 0 dBm input signal. It was also shown that the pump at 975 nm had a higher slope efficiency of 32% and an output power of more than 3.5 Watts at 1550 nm, while the 915 nm pump had a 11.5% slope efficiency and 1.5 Watt output power at 1550 nm [16].

One of the main difficulties in obtaining high powers out of amplifiers of a narrow linewidth signals are nonlinear effects such as the stimulated Brillouin scattering [17]. A description of a 1552 nm narrow linewidth CW signal being amplified, to an output power of 83 W using EYDF and all fiber distributed feedback (DFB) laser, is to be discussed. Figure 3.5 shows the different stages of this amplifier/laser.

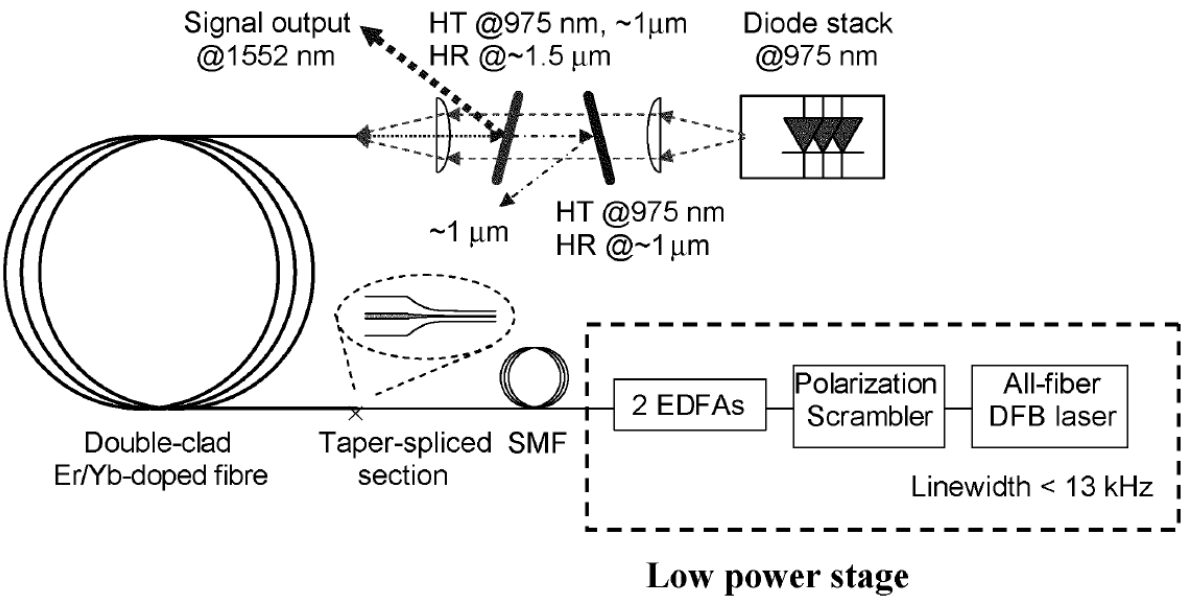

Figure 3.5: Experimental setup of high power amplifier. Reproduced from Ref. [11].

The narrow linewidth (13 kHz) seed consisted of a CW DFB fiber laser at 1552 nm and an output power of 10 mW. It was then polarization-scrambled using a commercial polarization controller. The low power amplifier stage was a chain of commercial amplifiers which boosted the signal to 2 watts output power. The final stage is the high power amplifier stage where a 3.5 m length of a dual-clad large-core EYDF was used. This EYDF was pumped with a high power diode stack operating at 975 nm which had its pump light focused onto the large core fiber. The slope efficiency of the amplifier was ~ 34% relative to the launched pump power. The linewidth of the 13- kHz single-frequency seed was not broadened after the three amplification stages. A maximum output power of 83 W was recorded with launching pump power of 250 W into the fiber [11].

3.2 **Pulsed high power laser amplifiers**

Many applications requires the laser emission to be in an eye-safe wavelength region in order to avoid an eye hazard, like free space communication, sensing or military ranging systems. In these cases, high power 1.5 μm wavelength sources are necessary which makes erbium/ytterbium co-doped fibers an excellent choice as a gain medium.

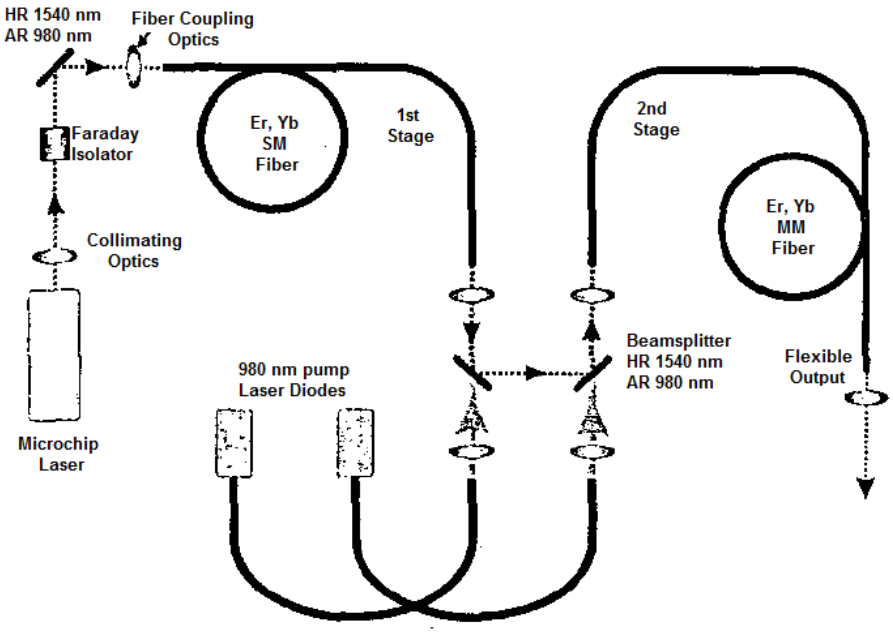

Figure 3.6: setup of the two-stage EYDFA. Reproduced from Ref. [18].

The figure above shows a set up of an amplifier based on EYDF's for a pulse signal at 1534nm. A passively Q-switched microchip laser is used. Pulses generated by the laser have a repetition rate of 800 Hz with short pulse duration of 4.5 ns. The pulsed laser is then collimated, isolated and then coupled into the first stage of the EYDF amplifier. In this stage the fiber is a single mode dual-clad fiber with a D-shaped inner cladding pumped by a temperature controlled laser diode. This laser diode gives a power of 1 W at 980 nm. A single mode output pulse energy of ~ 57 µJ at 1534 nm is delivered at this stage.

The output of the first stage is then coupled into the second EYDFA which is in return forwardly pumped with 2.12 Watts of power at 980 nm. Because of the higher pulse energy in the second stage a multi mode doped fiber is chosen here.

A 127 mW average signal power was achieved with this amplifier with a pulse repetition rate of 800 Hz and a pulse width of 4.5 ns. A peak pulse energy of 158 µJ was achieved which corresponds to 53 kW output pulsed power [18].

Another scheme was published in 2009, where figure 3.7 shows its schematics. A CW telecom laser diode, modulated externally, was used to seed the system with up to 1 mW.

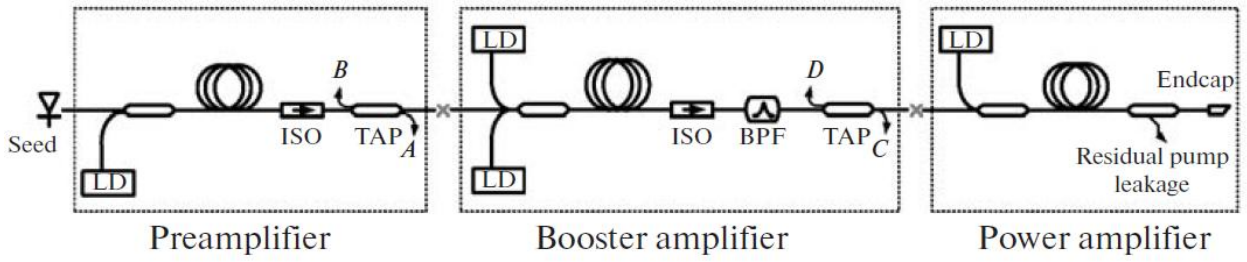

Figure 3.7: A three stage all-fiber cascaded amplifier. Reproduced from Ref. [19].

A high quality seeding source is important for achieving stable pulse energy and high optical signal-to-noise ratio (OSNR). The output signal was then amplified in a cascaded all fiber amplifier.

The first stage is the pre-amplifier using an EDF which gave a gain of 24 dB to the seed which corresponds to 250 mW. The other two stages of power amplifiers were built with dual-clad erbium/ytterbium co-doped fibers where they boost the signal up to 6 W. The EYDF in the second stage is a multi mode fiber with a core of 7 µm and a diameter of 130 µm for the inner cladding, while the EYDF in the third stage has a 25 µm diameter and an optical inner cladding of 300 µm in diameter. This fiber was pumped with up to 30 W.

A band pass filter was also used after the booster amplifier to suppress the ASE noise. At the end, an all; fiber pulse amplifier was built providing a power of 6 W and a signal peak over 50 dB above the background ASE [19].

3.3 **Summary**

We have seen the performance of different EYDFA's, a maximum power of CW light at 1552 nm was 83 W with a slope efficiency of ~ 34% relative to the launched pump power, which was at 975 nm. It was also shown from another setup that higher power and slope efficiency can be achieved when pumping at 975 nm verses pumping at 915 nm. EYDFA's are capable of amplifying light on a wide range of wavelengths from 1545 nm to 1570 nm.

It was also shown that EYDFA's work also for pulsed laser signals, amplifying them up to tens of kilowatts of peak power.

Chapter 4 - Experiment

The overall setup of the high power amplifier consists of two parts, a pre-amp and the power amplifier. The pre-amp is necessary to provide the signal for the power amplifier which is designed for an output of ~10 W at 1535 nm. Therefore, a relatively larger signal is needed which is about 200 mW.

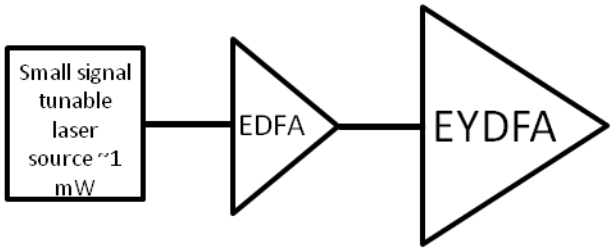

Figure 4.1: Schematic of the high power amplifier. EDFA: erbium doped fiber amplifier. EYDFA: erbium/ytterbium co-doped fiber amplifier.

A tunable laser source is used to give a signal of 1 mW. It goes through the EDFA which is the pre-amp, and finally through the EYDF amplifier which is the power amplifier.

Heat management is discussed at the end of this chapter. Since we are shooting for Watts of power, heat must be dissipated from the fiber to prevent the melting of its core.

4.1 **The pre-amplifier**

The first step for building the high power amplifier (HPA) was building the pre amp, such that the output of it will be seeding the HPA. A 2 m length of OFS EDF80 erbium doped fiber (EDF) was used as gain fiber. It is a single mode fiber with a core diameter of 125 µm doped with high erbium concentration. The setup of the pre-amp is described in the figure below.

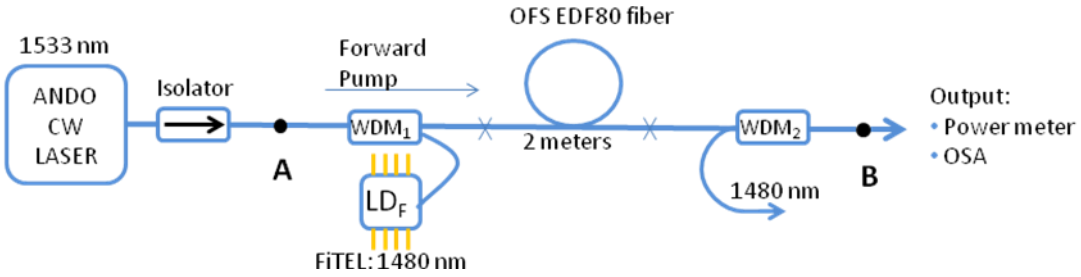

Figure 4.2: ANDO: a Continuous Wave laser source at 1533nm. $WDM_{1,2}$: Wavelength Division Multiplexer (1480nm/1550nm). LD_F: Laser Diode. OSA: Optical Spectral Analyzer.

The signal (at 1533nm) is propagating through Corning SMF-28e single mode fiber (SMF), the power going through point **A** is 1 µW for the small signal gain measurements and 1mW for the large signal gain measurements. The wavelength division multiplexor (WDM_1) allows both the signal and the pump to propagate through the gain fiber. The EDF is forward pumped using one 1480 nm semiconductor laser diode. WDM_2 is used to make sure that the light going through point **B** is of the signal's wavelength only. Any excess of the pump light (1480nm) exits the amplifier.

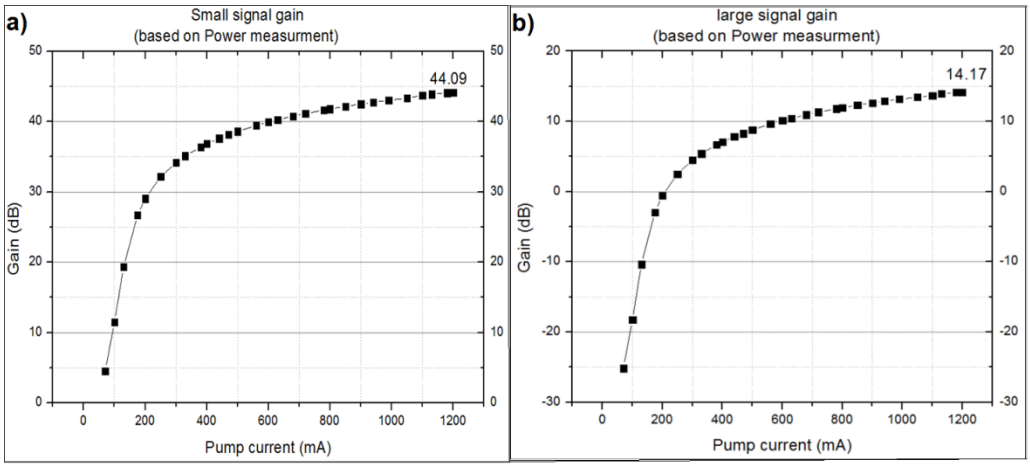

Figure 4.3: a) Small signal gain with input signal power of -31.94 dBm. B) Large signal gain with input signal power of 0.069 dBm.

A small signal gain of 44.09 dB and a large signal gain of 14.17 dBm was measured. Maximum output power was 28 mW for the small signal case.

For the attempt to get higher amplification I added three more segments of the same gain fiber (OFS EDF80), changed the pump light to 980 nm, and cut WDM_2 (since our pump light is now different). The EDF length now is 5.7 m instead of 2 m.

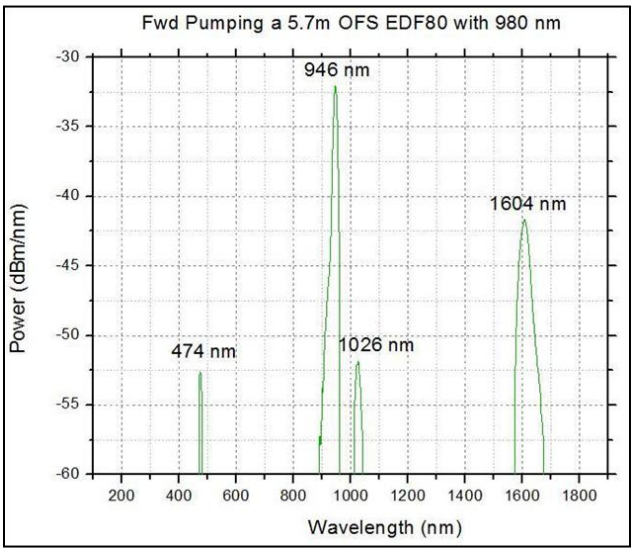

Figure 4.4: Spectrum of the output of a seeded 5.7m long Erbium doped fiber forwardly pumped with 980nm laser diode.

When looking at the output using the optical spectrum analyzer, we can see that both the pump and the signal light were being absorbed (Figure 4.4).

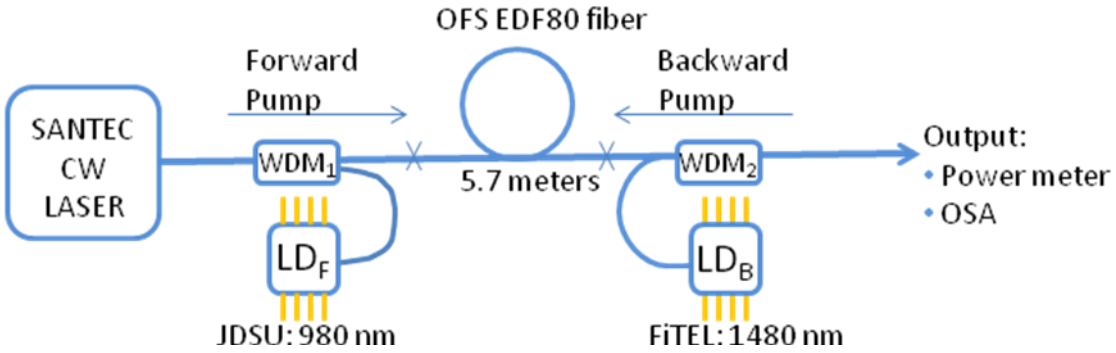

Figure 4.5 SANTEC: a tunable continuous wave laser source. $WDM_{1,2}$: Wavelength Division Multiplexer. LD_F: Laser Diode forward pumping the gain fiber. LD_B: Laser Diode backward pumping the gain fiber. OSA: Optical Spectral Analyzer. Power meter: to measure the total output power in mW.

Figure 4.5 shows the new setup for the pre amp, having a forward pump with 980 nm semiconductor laser diode and a backward pump using a 1480nm semiconductor laser diode, the 1480 nm light is propagating in the opposite direction as the signal, known as backward pumping. The output total power was 182 mW.

The output spectrum of the pre-amplifier was measured using an optical spectral analyzer. Since input was wavelength tunable, I was also able to change the signal's wavelength. The amplifier work best at 1560 nm since at this wavelength most of the amplifier power was in the signal and not in the ASE (Fig. 4.6).

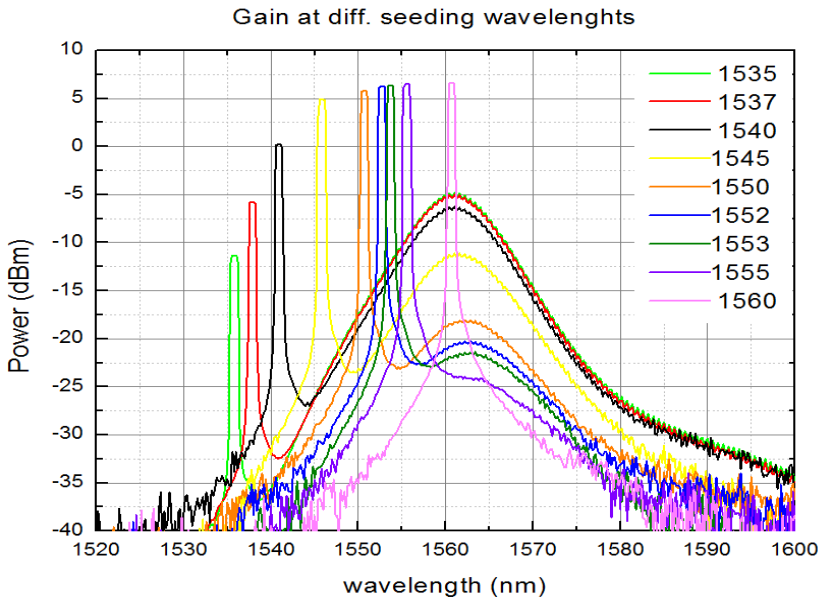

Figure 4.6: Power dependence on the seeding wavelength.

4.2 **Er/Yb doped fiber high power amplifier**

As mentioned earlier, the pre amp's output is to seed the high power amplifier, where the gain fiber is a dual-clad fiber doped with erbium and ytterbium. This fiber is being pumped with three power laser diodes operating at 915 nm. Each laser diode is designed to give a maximum power of 10 W, and for that they need to be driven by a high current control driver which can provide the power needed to operate these laser diodes.

4.2.1 Current Control of the pump laser diodes

The pump laser diodes were driven by a controller box that we have built. This controller box is a current controller where it goes up to 15 A. Since the pump laser diodes are suppose to give 10 W of power each, they will need to be driven at high currents. The following two figures show the schematic of the circuits that are designed in a way to control the output current and vary that from 0-15 A, which corresponds to the change of pump power from 0-10 W.

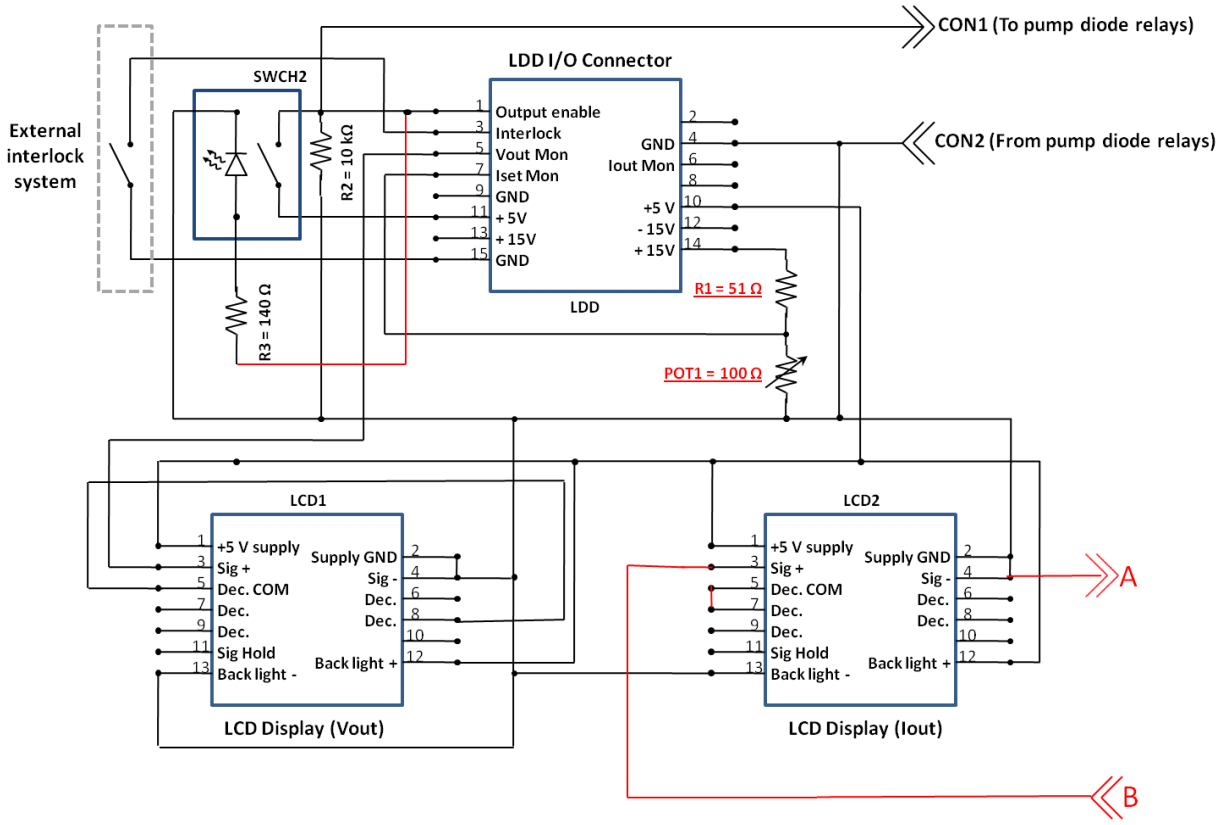

Figure 4.7: The electric circuit to control the current and display both the current (going through the laser diodes) and voltage (across them). Red color indicates any changes done to the original diagram. LCD: Liquid Crystal Display.

The laser diode diver (LDD) gives out a current up to 15 A at 10 V across its output. A voltage divider consisting of the two resistors R1 and POT1 (Fig. 4.7) are used to scale the voltage between pin-14 and pin-4 from 15 to 10 V. Using a potentiometer enables us to change the scaling factor such that the output voltage can range from 0 to 10 V; hence the output current can change from 0 to 15 A correspondingly. LCD1 and LCD2 are two displays; LCD1 is used to display the voltage across the output pins and LCD2 is to display the current going through the laser diodes.

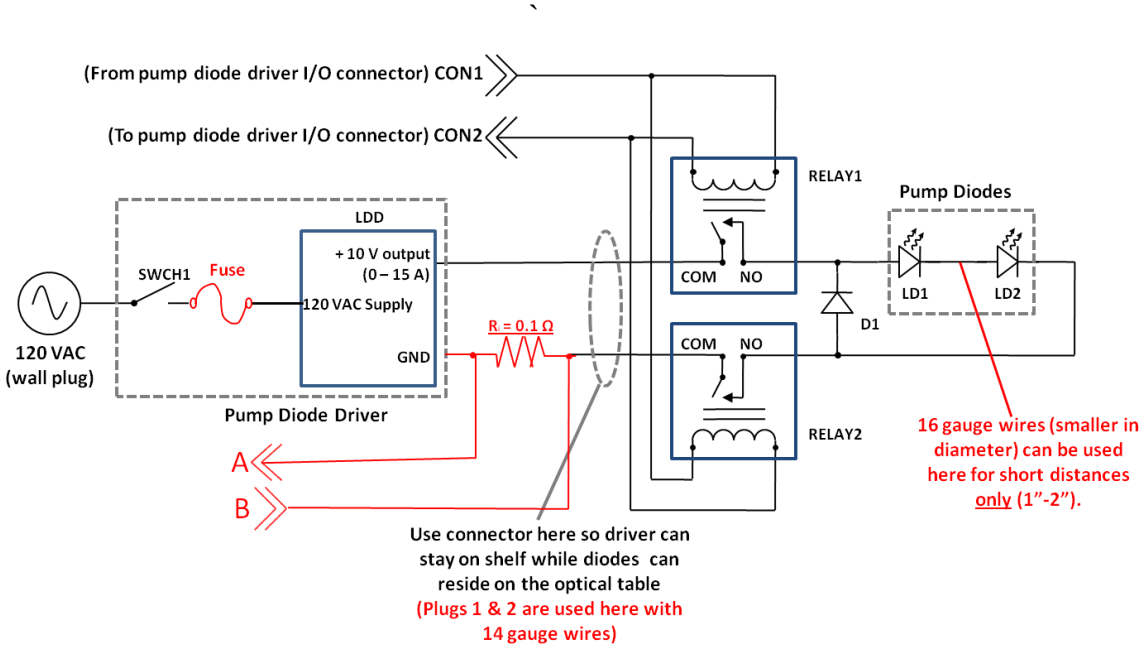

Figure 4.8: the Pump Diode Driver is the circuit (described in Figure 4.5) added to it a fuse and a switch. This diagram shows how the Pump Diode Driver is connected to a 120 Volts AC supply and to the laser diodes themselves. Red color indicates any changes done to the original diagram.

To measure the output current of the laser diode driver we installed the resister *R* of resistance 0.1Ω. The advantage of that was, voltage across *R* will be 0.1 times the current flowing through *R* (Ohm's law) hence by measuring voltage across *R* we measured *I*. With a proper decimal place which can be controlled, whatever current going through *R* will be displayed on the LCD2.

4.2.2 The Er^{3+} / Yb^{3+} Gain fiber

The CoreActive Er^{3+}/Yb^{3+} co-doped fiber is a dual-clad fiber, where the pump light is guided through the cladding instead of the core (Fig. 4.9). Co-doping with these two rare-earth metals provide highly efficient energy transfer and allows low cost, high power pumps.

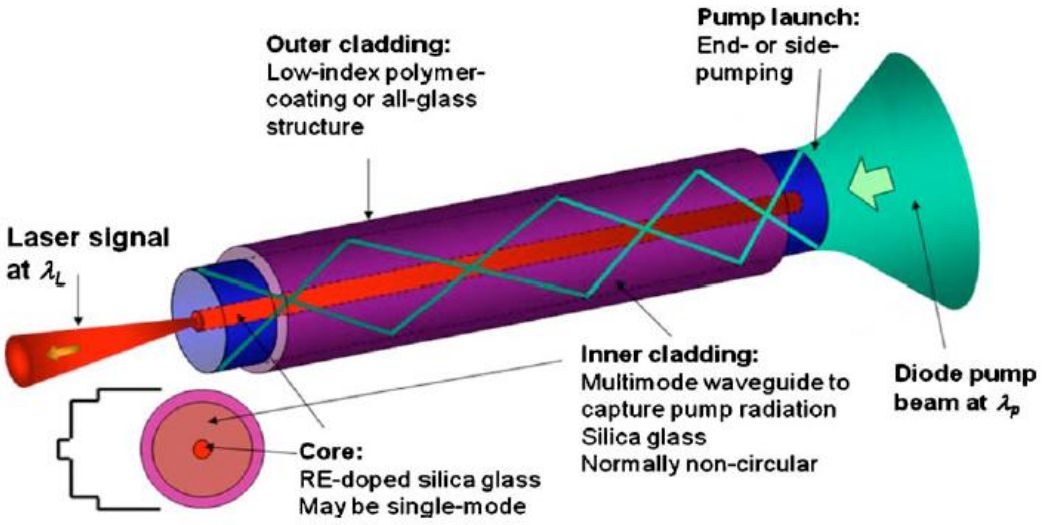

Figure 4.9: A diagram of a dual-clad fiber. The pump light propagates through the inner cladding while the signal propagates through the core. The diagram on the left corner shows the step index profile of the core, inner cladding and the outer cladding. Reproduced from Ref. [20].

The figure below shows the setup for the high power amplifier using the Er^{3+}/Yb^{3+} co-doped dual-clad fiber. The output of the pre-amplifier discussed earlier in this chapter is now the signal of this amplifier. About 180 mW at 1560 nm light going through an isolator, the high power coupler, and then the gain fiber which is being pumped with three laser diodes operating at 915 nm. Each of the laser diodes gives out a maximum of 10 W of light.

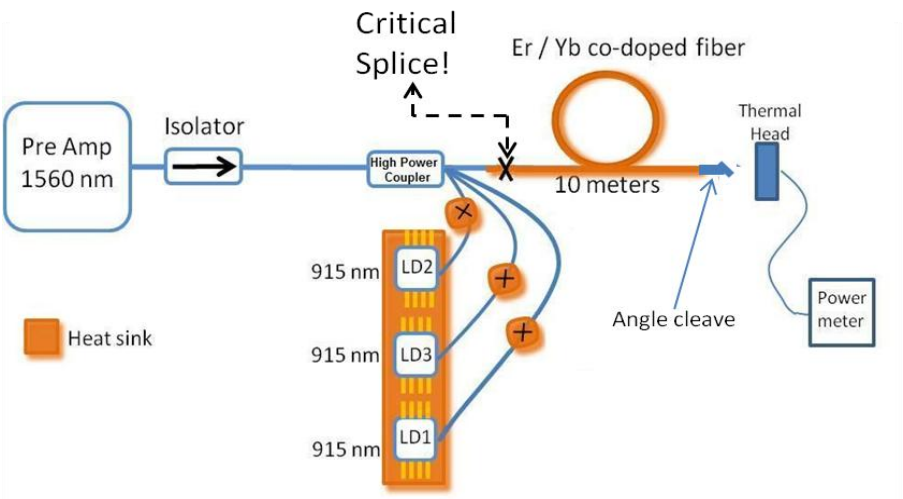

Figure 4.10: The Setup for the high power amplifier using Er/Yb co-doped fiber; pumped with three laser diodes and seeded with the output of the pre-amp.

Due to the high power of the combined pump light; the splice between the end of the coupler and the gain fiber is a critical splice, about 30 W of CW light needs to go through this splice with the minimum loss possible, which raises another issue of thermal energy which will be discussed in Section 4.3.

The couplers output fiber is a dual-clad fiber with 125 µm in diameter and a core of 8 µm roughly. However; the EYDF, which is also a dual-clad fiber, has a hexagonal shape with 125µm from one flat end to the other making it a bigger fiber than the couplers output fiber and a core size of 10 µm, add to that the difference of the core sizes these two factors contribute to the difficulty of making a good splice. We set the arc fusion splicer on manual mode to do the critical splice. An attempt to make an active alignment splice was made, but it failed due to the difference in the core sizes between the two fibers. There was a range of positions where the output of the active alignment is at its peak, so it was hard to determine through this method the best position at which to do the splice. With practice, we managed to make a good splice manually, where we moved the fibers close to each other trying to make their interface as close as we could to the middle of the screen of the splicer, then pushing the fusion button. The Er/Yb co-doped dual-clad fiber was angle cleaved at its output to protect the system from any back reflections at this interface. See figure 4.10.

The maximum output recorded of the high power amplifier was 1.6 W with slope efficiency ~ 11.25%. See Fig. 4.11.

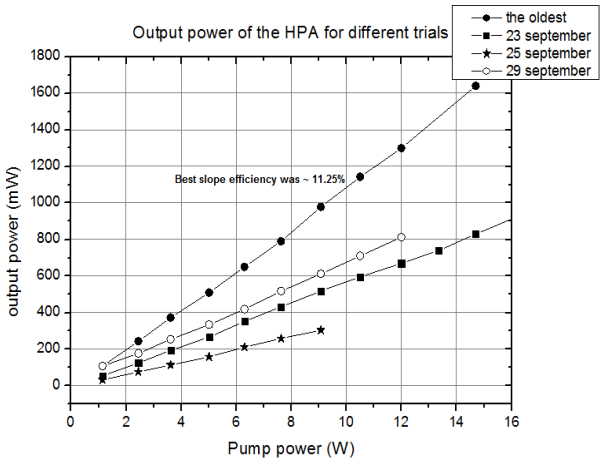

Figure 4.11: Output power from the EYDFA verses pump power

Other attempts failed due to multiple reasons, not having a good splice, recoating issues or heat not being dissipated very efficiently. Note that the pump power goes up to almost 30 W but due to poor heat sinking, the fiber melted at the splice point.

4.3 **Heat management**

Since we are dealing with tens of Watts of pump power, heat management here is crucial. If you look back at Figure 4.10, you'll notice where heat sinking is needed (in orange):

- The pump laser diodes:

  Mounted on top of an aluminum U shaped piece where a manifold is attached to its bottom. Anti freeze runs through this manifold and circulating through a chiller dumping the heat into it and keeping the laser diodes operating at a constant temperature (30 C^{o}).

- The splices between the three laser diodes and the coupler's input fibers:

  Each laser diode fiber is spliced to one of the coupler's input fibers. In order for the interface of the splice to handle a high power (~10W) we developed a heat sink for each splice. A small V-groove is cut in the middle of a 1"×1"

aluminum block. A heat shrink sleeve was put around the fiber before splicing, after the splice is done, hot air was blown to shrink the sleeves on each side of the cleave, and the fiber between the shrunk sleeves was covered with a heat sink compound. Then the fiber was inserted into a thin copper tube such that the splice is within the tube and the sleeves are partially coming out of the tubing. The rubber of the heat shrink sleeve is to protect the fiber from scratching against the metal tubing. This metal tube is then placed in the V-groove and covered with an aluminum cover that can be screwed to the aluminum block; which in turn is mounted to a cooling plate.

- The critical splice and the gain fiber:

  Starting with few centimeters before the critical splice (see Figure 4.7) and all the way to almost the end of the 10 m gain fiber, the fiber was wrapped around a metal can that was filled with water and placed on the same cooling plate. In this way both the splice and the rest of the gain fiber is allowed to dissipate heat.

Chapter 5 - Conclusions

We have built a pre-amp using an erbium doped fiber that operates at wavelengths between 1540 nm and 1560 nm. Since the efficiency of the current design of the pre-amp was best at 1560 nm, it was decided to work at this wavelength with an output of ~ 180 mW of signal light.

This pre-amp was then used to seed the high power amplifier which consists of Er/Yb co-doped fiber. The maximum recorded power output of this amplifier was 1.6 W. Our goal of achieving 10 W of CW light at 1535 nm was not met.

Since the absorption and the emission spectrums of the erbium ion overlap, it is believed that the erbium doped fiber is long enough such that the erbium ions are re-absorbing the light; therefore the spontaneous emission gets amplified. In order to amplify the light through the pre-amp at lower wavelengths (~1535 nm) some cut back measurements need to be done.

For the high power part of this amplifier, better heat sinking methods needs to be established, especially the heat sinking of the gain fiber at the critical splice.

A search in the literature was done of the existing EYDFA's. It was shown that these co-doped amplifiers work for the continuous or pulsed wave. These amplifiers amplify the signals up to peak powers of 83 Watts for a continuous wave signal and up to kilowatts for pulsed signals. It was also shown that these amplifiers work on a wide range of wavelengths around 1550 nm.

References

1. W. Rudolph, A. V. V. Nampoothiri, A. Ratanavis, A. Jones, R. Kadel, B. R. Washburn, K. L. Corwin, N. Wheeler, F. Couny, and F. Benabid, "Mid-IR laser emission from a C2H2 gas filled hollow core fiber," in *Transparent Optical Networks (ICTON), 2010 12th International Conference on*, Anonymous (, 2010), pp. 1-4.
2. W. C. Swann, "Pressure-induced shift and broadening of 1510-1540-nm acetylene wavelength calibration lines," Journal of the Optical Society of America.B, Optical physics **17,** 1263-70 (2000).
3. M. W. Wright and G. C. Valley, "Yb-doped fiber amplifier for deep-space optical communications," Lightwave Technology, Journal of **23,** 1369-1374 (2005).
4. D. Anthon, J. Fisher, M. Keur, K. Sweeney, D. Ott, P. Maton, and C. Emslie, "High power optical amplifiers for CATV applications," in *Optical Fiber Communication Conference and Exhibit, 2001. OFC 2001*, Anonymous (, 2001), pp. TuI1-TuI1.
5. J. T. Verdeyen, Laser Electronics, (Prentice Hall Series in Solid State Physical Elecronics,1995), p.376-377
6. http://people.seas.harvard.edu/~jones/ap216/lectures/ls_2/ls2_u5/ls2_unit_5.html
7. W. H. Hayt, Engineering Elecromagnetics, McGraw-Hill Series in Electrical Engineering, 2005.
8. A. E. Siegman, Lasers, edited by A. Kelly (University Science Books, Sausalito, CA, 1986), p.297-300
9. A. Carter, "Damage mechanisms in components for fiber lasers and amplifiers," Proceedings of SPIE--the international society for optical engineering **5647,** 561-71 (2005).
10. K. Aiso, "Development of Er/Yb Co-doped fiber for high-power optical amplifiers," FURUKAWA REVIEW41-45 (2001).
11. C. Alegria, Y. Jeong, C. Codemard, J.K. Sahu, J.A. Alvarez-Chavez, L. Fu, M. Ibsen, and J. Nilsson, "83-W single-frequency narrow-linewidth MOPA using large-core erbium-ytterbium Co-doped fiber," Photonics Technology Letters, IEEE **16,** 1825-1827 (2004).

12. J. Hansryd and P. A. Andrekson, "Broadband CW pumped fiber optical parametric amplifier with 49 dB gain and wavelength conversion efficiency," in *Optical Fiber Communication Conference, 2000*, Anonymous (, 2000), pp. 175-177 vol.4.
13. http://www.fibercore.com/LinkClick.aspx?fileticket=-HKV3TPiUlo%3D&tabid=68&mid=619
14. N. Park, P. Wysocki, R. Pedrazzani, S. Grubb, D. DiGiovanni, and K. Walker, "High-power Er-Yb-doped fiber amplifier with multichannel gain flatness within 0.2 dB over 14 nm," Ieee Photonics Technology Letters **8,** 1148-1150 (1996).
15. L. Goldberg and J. Koplow, "High power side-pumped Er/Yb doped fiber amplifier," in *Optical Fiber Communication Conference, 1999, and the International Conference on Integrated Optics and Optical Fiber Communication. OFC/IOOC '99. Technical Digest*, Anonymous (, 1999), pp. 19-21 vol.2.
16. P. R. Kaczmarek, T. Rogowski, E. Kopczynski, P. Karnas, and K. M. Abramski, "High output power Erbium-Ytterbium doped fibre amplifier," in *Transparent Optical Networks, 2008. ICTON 2008. 10th Anniversary International Conference on*, Anonymous (, 2008), pp. 350-352.
17. I. Dajani, "Investigation of nonlinear effects in multitone-driven narrow-linewidth high-power amplifiers," IEEE journal of selected topics in quantum electronics **15,** 406 (2009).
18. F. Imkenberg, J. Barenz, H. D. Tholl, A. Malinowski, K. Furusawa, and D. J. Richardson, "Microchip laser master-oscillator Er/Yb-doped fiber-power-amplifier emitting 158 μJ pulses with a duration of 4.5 ns," in *Lasers and Electro-Optics Europe, 2003. CLEO/Europe. 2003 Conference on*, Anonymous (, 2003), pp. 628.
19. B. Peng, H. Zhang, M. Gong, and P. Yan, "All-Fiber Eye-Safe Pulsed Laser with Er-Yb Co-Doped Multi-Stage Amplifier," Laser Physics **19,** 2019-2022 (2009).
20. D. J. Richardson, "High power fiber lasers: current status and future perspectives," Journal of the Optical Society of America.B, Optical physics **27,** B63-B92 (2010).
21. A. E. Siegman, Lasers, edited by A. Kelly (University Science Books, Sausalito, CA, 1986), p.266-272
22. E. Desurvire and J. R. Simpson, "Amplification of spontaneous emission in erbium-doped single-mode fibers," Lightwave Technology, Journal of **7,** 835-845 (1989).

23. E. Desurvire and J. R. Simpson, "Amplification of spontaneous emission in erbium-doped single-mode fibers," Lightwave Technology, Journal of **7,** 835-845 (1989).